

Barrierless Electron Transfer Bond Fragmentation Reactions

Edward D. Lorange, Wolfgang H. Kramer, and Ian R. Gould*

Contribution from the Department of Chemistry and Biochemistry, Arizona State University, Tempe, Arizona 85287-1604

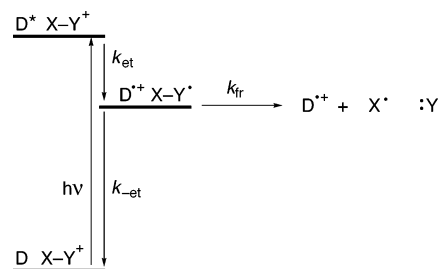
Received July 17, 2003; E-mail: igould@asu.edu

Abstract: The ultrafast N–O bond fragmentation in a series of *N*-methoxy-pyridyl radicals, formed by one-electron reduction of the corresponding *N*-methoxy-pyridiniums, has been investigated as potentially barrierless electron-transfer-initiated chemical reactions. A model for the reaction involving the electronic and geometric factors that control the shape of the potential energy surface for the reaction is described. On the basis of this model, molecular structural features appropriate for ultrafast reactivity are proposed. Femtosecond kinetic measurements on these reactions are consistent with a kinetic definition of an essentially barrierless reaction, i.e., that the lifetime of the radical is a few vibrational periods of the fragmenting bond, for the *p*-methoxy-*N*-methoxy-pyridyl radical.

Introduction

Bond fragmentation upon one-electron oxidation or reduction is of both mechanistic¹ and technological interest.² In particular, reactions of radical anions formed upon one-electron reduction have been studied as paradigm bond-breaking processes.^{3,4} Also of interest in photochemical processes has been the development of very fast fragmentation reactions,⁵ the importance of which is illustrated in Scheme 1. In this example, exothermic electron transfer (k_{et}) occurs from an excited donor (D) to a positively charged electron acceptor X–Y⁺ to form the donor radical cation, D⁺, and a radical X–Y[•]. Fragmentation of this radical to form a new radical X[•] and a neutral molecule Y (k_{fr}) occurs

Scheme 1



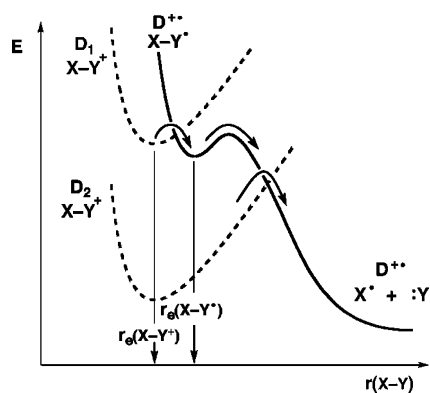
in competition with return electron transfer ($k_{-\text{et}}$). Clearly, the larger k_{fr} , the less energy-wasting return electron transfer occurs. Ideally, the fragmentation reaction, k_{fr} , should be so fast that it occurs in concert with electron attachment and with no barrier. An obvious question is how can such concerted and barrierless reactions be designed?

The dissociative electron-transfer reactions of alkyl and aryl halide and other radical anions provide the most useful guide.^{4,6} The usual thermodynamic cycle description of redox-activated bond cleavage predicts that, for a series of otherwise equal molecules, fragmentation of a radical anion should become more energetically favorable with increasingly negative reduction potential of the parent molecule and thus presumably be faster.⁷

- (1) See, for example: (a) Maslak, P. *Top. Curr. Chem.* **1993**, *168*, 1. (b) Saveant, J.-M. *Acc. Chem. Res.* **1993**, *26*, 455. (c) Albini, A.; Fasani, E.; d'Alessandro, N. *Coord. Chem. Rev.* **1993**, *125*, 269. (d) Saveant, J.-M. *Adv. Electron-Transfer Chem.* **1994**, *4*, 53. (e) Gaillard, E. R.; Whitten, D. G. *Acc. Chem. Res.* **1996**, *29*, 292.
- (2) (a) Crivello, J. V. *Adv. Polym. Sci.* **1984**, *62*, 1. (b) Reiser, A. *Photoreactive Polymers, the Science and Technology of Resists*; Wiley: New York, 1989. (c) Saeva, F. D. *Top. Curr. Chem.* **1990**, *156*, 59. (d) DeVoe, R. J.; Olofson, P. M.; Sahyun, M. R. V. *Adv. Photochem.* **1992**, *17*, 313. (e) Saeva, F. D. *Adv. Electron-Transfer Chem.* **1994**, *4*, 1. (f) Paczkowski, J.; Neckers, D. C. In *Electron Transfer in Chemistry*; Balzani, V., Ed.; Wiley-VCH: New York, 2001; Vol. 5, p 516. (g) Gould, I. R.; Shukla, D.; Giessen, D.; Farid, S. *Helv. Chim. Acta* **2001**, *84*, 2796.
- (3) (a) Parker, V. D. *Acta Chem. Scand. B* **1981**, *B35*, 595. (b) Hammerich, O.; Parker, V. D. *Acta Chem. Scand. B* **1981**, *B37*, 851. (c) Koppang, M. D.; Woolsey, N. F.; Bartak, D. E. *J. Am. Chem. Soc.* **1985**, *107*, 4692. (d) Maslak, P.; Guthrie, R. D. *J. Am. Chem. Soc.* **1986**, *108*, 2628. (e) Maslak, P.; Narvaez, J. N. *Angew. Chem.* **1990**, *4*, 302. (f) Ruhl, J. C.; Evans, D. H.; Hapiot, P.; Neta, P. *J. Am. Chem. Soc.* **1991**, *113*, 5188. (g) Wu, F.; Guarr, T. F.; Guthrie, R. D. *J. Phys. Org. Chem.* **1992**, *5*, 7. (h) Saveant, J. M. *J. Phys. Chem.* **1994**, *98*, 3716. (i) Guthrie, R. D.; Patwardhan, M.; Chateaufneuf, J. E. *J. Phys. Org. Chem.* **1994**, *7*, 147. (j) Mathivanan, N.; Johnston, L. J.; Wayner, D. D. M. *J. Phys. Chem.* **1995**, *99*, 8190. (k) Maslak, P.; Theroff, J. *J. Am. Chem. Soc.* **1996**, *118*, 7235. (l) Andrieux, C. P.; Saveant, J.-M.; Tallec, A.; Tardivel, R.; Tardy, C. *J. Am. Chem. Soc.* **1996**, *118*, 9788. (m) Andrieux, C. P.; Combellas, C.; Kanoufi, F.; Saveant, J.-M.; Thiebault, A. *J. Am. Chem. Soc.* **1997**, *119*, 9527. (n) Benassi, R.; Bertarini, C.; Taddei, F. *J. Chem. Soc., Perkin Trans. 2* **1997**, 2263. (o) Borsari, M.; Fontanesi, C.; Gavioli, G. *Curr. Top. Electrochem.* **1997**, *5*, 167. (p) Zheng, Z.-R.; Evans, D. H.; Chan-Shing, E. S.; Lessard, J. J. *Am. Chem. Soc.* **1999**, *121*, 9429. (q) Eberson, L. *Acta Chem. Scand.* **1999**, *53*, 751. (r) Beregovaya, I. V.; Shchegoleva, L. N. *Chem. Phys. Lett.* **2001**, *348*, 501. (s) Andrieux, C. P.; Farriol, M.; Gallardo, L.; Marquet, J. *J. Chem. Soc., Perkin Trans. 2* **2002**, 985. (t) Costentin, C.; Robert, M.; Saveant, J.-M. *J. Am. Chem. Soc.* **2003**, *125*, 105.

- (4) See, for example: (a) Andrieux, C. P.; Le Gorande, A.; Saveant, J.-M. *J. Am. Chem. Soc.* **1992**, *114*, 6892. (b) Grimshaw, J.; Langan, J. R.; Salmon, G. A. *J. Chem. Soc., Faraday Trans* **1994**, *90*, 75. (c) Andrieux, C. P.; Robert, M.; Saeva, F. D.; Saveant, J.-M. *J. Am. Chem. Soc.* **1994**, *116*, 7864. (d) Saveant, J.-M. *Adv. Electron-Transfer Chem.* **1994**, *4*, 53. (e) Adcock, W.; Andrieux, C. P.; Clark, C. I.; Neudeck, A.; Saveant, J.-M.; Tardy, C. *J. Am. Chem. Soc.* **1995**, *117*, 8285. (f) Andrieux, C. P.; Saveant, J.-M.; Tallec, A.; Tardivel, R.; Tardy, C. *J. Am. Chem. Soc.* **1997**, *119*, 2420. (g) Andrieux, C. P.; Saveant, J.-M.; Tardy, C. *J. Am. Chem. Soc.* **1997**, *119*, 11546. (h) Zhong, D.; Zewail, A. H. *Proc. Natl. Acad. Sci. U.S.A.* **1999**, *96*, 2602. (i) Costentin, C.; Hapiot, P.; Medebielle, M.; Saveant, J.-M. *J. Am. Chem. Soc.* **2000**, *122*, 5623. (j) Pause, L.; Robert, M.; Saveant, J.-M. *J. Am. Chem. Soc.* **2000**, *122*, 9829. (k) Soriano, A.; Silla, E.; Tunon, I. *J. Chem. Phys.* **2002**, *116*, 6102. (l) Antonello, S.; Crisma, M.; Formaggio, F.; Moretto, A.; Taddei, F.; Toniolo, C.; Maran, F. *J. Am. Chem. Soc.* **2002**, *124*, 11503. (m) Cardinale, A.; Isse, A. A.; Gennaro, A.; Robert, M.; Saveant, J.-M. *J. Am. Chem. Soc.* **2002**, *124*, 13533.

Scheme 2



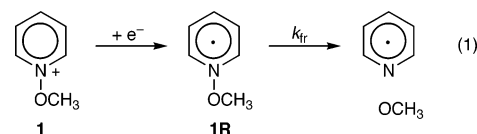
This prediction has been confirmed by experiment, especially in the benzyl halide series.⁶ Although some time-resolved measurements have been reported,⁸ these reactions have mainly been studied using electrochemical methods.⁴ The electrochemical time scale, however, is slow compared to that of the fastest possible fragmentation reactions, and this has led to some questions about the nature of very fast dissociative processes, particularly when results of electrochemical and photochemical processes are compared.^{9–12}

The principle issues seem to be the definition of a concerted dissociative reaction and whether this implies that the fragmentation process occurs without any barrier. A kinetic definition of a truly barrierless reaction might be that the reduced (or oxidized) species has a lifetime of only one or two vibrational periods of the fragmenting bond. An alternative thermodynamic definition would be that this species has no potential energy minimum with respect to the fragmentation coordinate. In a series of detailed investigations of such processes, however, Saveant has clearly shown that the thermodynamics of the initial electron-transfer process has to be considered when asking questions such as these.¹³ Consider Scheme 2, which shows

energy diagrams for electron transfer from two different donors, D_1 and D_2 , to a fragmentable acceptor, $X-Y^+$, as a function of the $X-Y$ separation distance, $r(X-Y)$. The dashed curves represent the energies of the donor/acceptor pairs before electron transfer and have minima at the equilibrium bond distance of the $X-Y^+$, $r_e(X-Y^+)$. D_1 is a stronger electron donor than D_2 , and thus the dashed curve for this pair is higher in energy. The energy curve for fragmentation of the $X-Y^*$ formed by electron transfer from the donors shows exothermic fragmentation over a small barrier. Electron transfer from D_1 to $X-Y^+$ to form $X-Y^*$ at its equilibrium geometry, $r_e(X-Y^*)$, is exothermic and occurs at the crossing point of the upper dashed and solid curves as indicated. Fragmentation of the intermediate $X-Y^*$ subsequently occurs over the small barrier, again as indicated. Electron transfer from D_2 to $X-Y^+$ to form $X-Y^*$ at its equilibrium geometry is endothermic. Electron transfer to $X-Y^+$ occurs by stretching the $X-Y$ bond until the lower dashed curve and the solid curve cross as indicated. At this point the solid curve is repulsive with respect to the $X-Y$ bond. The overall reductive cleavage path for D_2 is obviously concerted because it involves only one transition state, but it is also clearly not barrierless. Indeed, reduction by D_2 may be characterized by a sufficiently large barrier (the crossing point of the lower dashed and the solid curves) to be essentially useless in a photochemical process.

Thus, for cleavage to proceed via the smallest energy barrier, electron transfer using a reductant such as D_1 is necessary. This would also allow the complete fragmentation energy surface of the reactive species to be explored, since $X-Y^*$ is formed at a geometry in which the energy curve is still in the attractive region. In this way, the factors controlling the barrier to fragmentation on the solid energy curve could be studied. The use of a photochemical reductant D_1 would also allow increased time resolution compared to electrochemical methods. Indeed, Ebersson has previously pointed to the need for experiments with femtosecond time resolution to address the problem of barrierless reactions.¹⁰ Such experiments form the basis of the present work.

We recently reported on rate constants for N–O bond fragmentation in a series of *N*-methoxyheterocycle radicals formed by one-electron reduction of the corresponding *N*-methoxy compounds (corresponding to $X-Y^+$), as illustrated in eq 1 for the case of the parent pyridinium, **1**.^{14,15} One-electron



reduction of **1** forms the pyridyl radical **1R** (corresponding to $X-Y^*$), which undergoes fragmentation to form the neutral pyridine and a methoxy radical. A wide range of rate constants was determined for these reactions, depending upon the particular *N*-methoxyheterocycle,¹⁴ and we wondered if it would be possible to rationally increase the rate constant for fragmentation toward the barrierless limit. Here we describe further

- (5) (a) Maslak, P.; Kula, J.; Chateaufeuf, J. E. *J. Am. Chem. Soc.* **1991**, *113*, 2304. (b) Zou, C.; Miers, J. B.; Ballew, R. M.; Dlott, D. D.; Schuster, G. B. *J. Am. Chem. Soc.* **1991**, *113*, 7823. (c) Perrier, S.; Sankaraman, S.; Kochi, J. K. *J. Chem. Soc., Perkin Trans. 2* **1993**, 825. (d) Lucia, L. A.; Wang, Y.; Nafisi, K.; Netzel, T. L.; Schanze, K. S. *J. Phys. Chem.* **1995**, *99*, 11801. (e) Maslak, P.; Narvaez, J. N.; Vallombroso, T. M., Jr. *J. Am. Chem. Soc.* **1995**, *117*, 12373. (f) Hassoon, S.; Sarker, A.; Polykarov, A. Y.; Rodgers, M. A. J.; Neckers, D. C. *J. Phys. Chem.* **1996**, *100*, 12386. (g) Bockman, T. M.; Hubig, S. M.; Kochi, J. K. *J. Org. Chem.* **1997**, *62*, 2110. (h) Bockman, T. M.; Hubig, S. M.; Kochi, J. K. *J. Am. Chem. Soc.* **1998**, *120*, 6542. (i) Rasmusson, M.; Akesson, E.; Ebersson, L.; Sundstrom, V. *J. Phys. Chem.* **2001**, *105*, 2027. (j) Nath, S.; Singh, A. K.; Palit, D. K.; Sapre, A. V.; Mittal, J. P. *J. Phys. Chem. A* **2001**, *105*, 7151.
- (6) For a summary, see ref 4d.
- (7) (a) Popielarz, R.; Arnold, D. R. *J. Am. Chem. Soc.* **1990**, *112*, 3068. (b) Maslak, P.; Vallombroso, T. M.; Chapman, W. H., Jr.; Narvaez, J. N. *Angew. Chem., Int. Ed. Engl.* **1994**, *33*, 73. (c) Wayner, D. D. M.; Parker, V. D. *Acc. Chem. Res.* **1993**, *26*, 287.
- (8) (a) Neta, P.; Behar, D. *J. Am. Chem. Soc.* **1980**, *102*, 4798. (b) Neta, P.; Behar, D. *J. Am. Chem. Soc.* **1981**, *103*, 103. (c) Behar, D.; Neta, P. *J. Am. Chem. Soc.* **1981**, *103*, 2280. (d) Norris, R. K.; Barker, S. D.; Neta, P. *J. Am. Chem. Soc.* **1984**, *106*, 3140. (e) Kimura, N.; Takamuku, S. *Bull. Chem. Soc. Jpn.* **1986**, *59*, 3653. (f) Kimura, N.; Takamuku, J. *J. Am. Chem. Soc.* **1995**, *117*, 8023.
- (9) (a) Shaik, S.; Danovich, D.; Sastry, G. N.; Ayala, P. Y.; Schlegel, H. B. *J. Am. Chem. Soc.* **1997**, *119*, 9237. (b) Robert, M.; Saveant, J.-M. *J. Am. Chem. Soc.* **2000**, *122*, 514.
- (10) Ebersson, L. *Acta Chem. Scand.* **1999**, *53*, 751.
- (11) Wang, X.; Saeva, F. D.; Kampmeier, J. A. *J. Am. Chem. Soc.* **1999**, *121*, 4364.
- (12) Pause, L.; Robert, M.; Saveant, J.-M. *ChemPhysChem* **2000**, *1*, 199.
- (13) These ideas are discussed in many papers from the Saveant group, including refs 4c,d,g,j,m and (a) Andrieux, C. P.; Merz, A.; Saveant J.-M. *J. Am. Chem. Soc.* **1985**, *107*, 6097. (b) Constantin, C.; Hapiot, P.; Medebielle, M.; Saveant, J.-M. *J. Am. Chem. Soc.* **1999**, *121*, 4451. (c) Pause, L.; Robert, M.; Saveant, J.-M. *J. Am. Chem. Soc.* **1999**, *121*, 7158. (d) Constantin, C.; Robert, M.; Saveant, J.-M. *J. Phys. Chem.* **2000**, *104*, 7492.

(14) Lorance, E. D.; Kramer, W. H.; Gould, I. R. *J. Am. Chem. Soc.* **2002**, *124*, 15225.

(15) See also similar work by Kochi et al.: (a) Lee, K. Y.; Kochi, J. K. *J. Chem. Soc., Perkin Trans. 2* **1992**, 1011. (b) Bockman, T. M.; Lee, K. Y.; Kochi, J. K. *J. Chem. Soc., Perkin Trans. 2* **1992**, 1581.

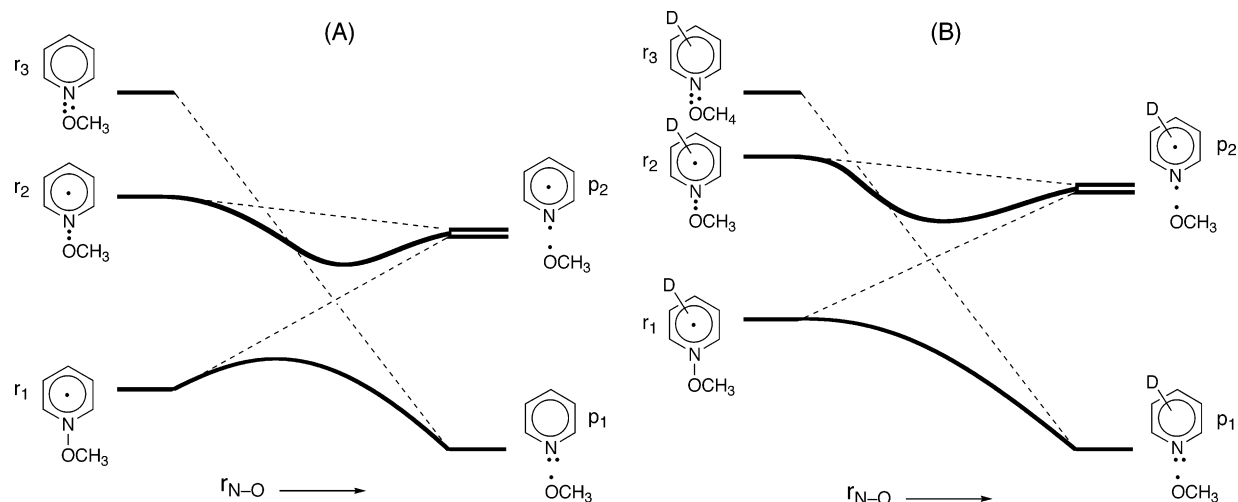
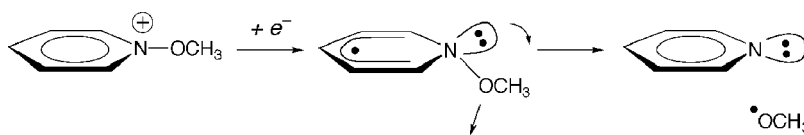


Figure 1. Correlation diagrams for cleavage of (A) unsubstituted *N*-methoxy pyridyl radical and (B) a corresponding radical substituted with a strong electron-donating group, D. The dots represent electrons not involved in pairwise bonding. Three reactant (r_1 – r_3) and product configurations (p_1 and a doubly degenerate p_2) are important; see text for their description. The dotted lines represent diabatic correlations in the planar radical, and the curves represent adiabatic potential energy surfaces formed upon configuration mixing in the nonplanar radicals in *N*-methoxyheterocycle radicals.

Scheme 3



studies on the N–O bond fragmentation reaction. A more detailed theoretical analysis of the N–O bond fragmentation process than given previously is discussed,¹⁴ and femtosecond kinetic methods for the study of fragmentation reactions of this type are described.

Theoretical Model for Bond Fragmentation

A qualitative state energy diagram of N–O bond cleavage for reduction of the parent *N*-methoxypyridinium compound is shown in Figure 1A. Addition of an electron results in the formation of the pyridyl radical (r_1 , Figure 1A). The electron is accepted into the lowest energy orbital, in this case a π^* orbital of the pyridyl system. However, increasing the N–O bond distance diabatically in a planar radical with this electronic configuration simply raises the energy of the electrons associated with the N–O σ bond and leads to the methoxy radical and an $n\text{-}\pi^*$ excited state of pyridine (p_2), rather than the ground-state pyridine and methoxy radical products (p_1). As discussed previously,¹⁴ certain electronic configurations of the radical involving population of the N–O σ^* orbital decrease in energy with increasing N–O bond distance. One obvious excited-state contributor has one electron in the π^* and two unpaired electrons, one in each of the σ and σ^* orbitals (r_2). Increasing the N–O bond distance in this planar radical produces the same pyridine $n\text{-}\pi^*$ excited state at infinite N–O separation as the ground state. Another, in which the N–O σ orbital has one electron and the σ^* orbital is doubly occupied (r_3), is also repulsive with respect to the N–O coordinate and when planar can form the ground-state products.

Thus, a barrier is predicted for fragmentation of the initially formed π^* pyridyl radical, corresponding to the energy required to attain the crossing point of the dotted lines originating with the r_1 and r_3 configurations in the correlation diagram. According to these diabatic correlations, however, the reaction will never

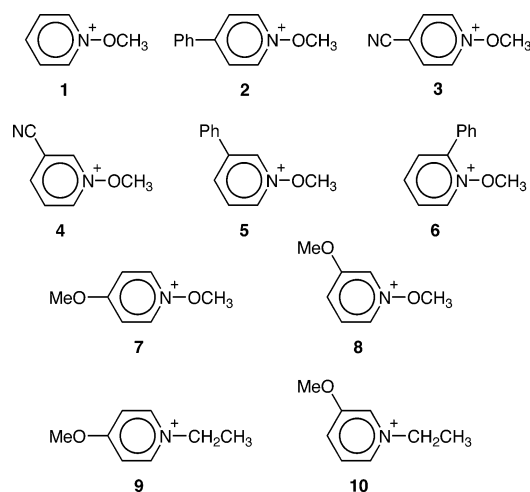
be barrierless. Consider the situation in Figure 1B. An electron-donating group affects mainly the energy of the π^* orbital, raising the energies of those configurations in which the π^* orbital is occupied, i.e., r_1 , r_2 , and p_2 . As indicated, this has the effect of increasing the reaction exothermicity and decreasing but not eliminating the energy of the diabatic crossing. The barrier only disappears in the unlikely situation that the energy of p_2 becomes lower than r_1 .

Mixing of either the reactant excited configuration r_3 with the reactant ground-state r_1 , or mixing the excited configurations r_2 and r_3 with each other, is symmetry forbidden when the radical is planar. Mixing as a function of N–O bond bending, however, generates adiabatic electronic states (solid lines in Figure 1).¹⁶ This feature is common to many bond-breaking reactions in which the ring symmetry plane must be broken to allow the mixing of the otherwise orthogonal σ and π systems.^{17–19} Of particular interest in this regard is the recent work by Hynes et al., who described fragmentation of the radical anion of *p*-cyanophenyl chloride in terms of stretching and out-of-plane bending of the C–Cl bond.¹⁸

Bending the N–O bond out of the plane of the ring is thus an important part of the reaction, Scheme 3. Indeed, we previously showed that all of the *N*-methoxyheterocycle radicals are bent at the local radical minimum, with increased bending

- (16) (a) Salem, L. *Electrons in Chemical Reactions*; Wiley-Interscience: New York, 1982. (b) Michl, J.; Bonacic-Koutecky, V. *Electronic Aspects of Organic Photochemistry*; Wiley-Interscience: New York, 1990. (c) Shaik, S. S.; Schlegel, H. B.; Wolfe, S. *Theoretical Aspects of Physical Organic Chemistry*; Wiley: New York, 1992. (d) Pross, A. *Theoretical and Physical Principles of Organic Chemistry*; Wiley: New York, 1995.
- (17) (a) Pearson, R. G. *Symmetry Rules for Chemical Reactions*; Wiley: New York, 1976; Chapter 5. (b) Reference 16b, Chapter 3.
- (18) (a) Laage, D.; Burghardt, I.; Sommerfeld, T.; Hynes, J. T. *ChemPhysChem* **2003**, *4*, 61. (b) Laage, D.; Burghardt, I.; Sommerfeld, T.; Hynes, J. T. *J. Phys. Chem. A* **2003**, *107*, 11271. (c) Burghardt, I.; Laage, D.; Hynes, James T. *J. Phys. Chem. A* **2003**, *107*, 11292.
- (19) Note that in a nonplanar conformation and in the absence of mixing, the r_2 state now correlates with the p_1 .

Scheme 4



being associated with increased reaction rate constant.¹⁴ An important additional consequence for the correlations of Figure 1B is that when mixing is extensive and the reaction is sufficiently exothermic, the splitting of the adiabats can potentially *eliminate* the barrier to reaction. This indicates that some combination of large reaction exothermicity and extensive configuration mixing by bending could be used to design a truly barrierless reaction.

This description of the reaction provides a more detailed understanding in terms of the important orbital energies than a simple thermodynamic cycle approach⁷ and allows more subtle substituent effects to be predicted. In addition to lowering the energy crossing point of the diabats, an electron-donating substituent in the *p*-position of the pyridyl should result in increased σ^* character as a consequence of state mixing, a lower activation energy, earlier transition state, and faster rate. An electron-withdrawing substituent on the pyridyl ring will lower the energy of the r_1 , r_2 , and p_2 , decreasing the σ^* character, resulting in less bending and a decreased rate. A delocalizing substituent such as an aromatic group will have the effect of lowering the energy of the π^* orbital, decreasing σ^* character, and reducing the reaction rate compared to the simple pyridyl system.

Structures and Experimental Approach

Consistent with this orbital and state picture of the reaction, the previous work on the substituted pyridyl radicals clearly indicated a decrease in rate constant for fragmentation with increasing delocalization and, more importantly, the use of electron-withdrawing groups.¹⁴ Illustrative examples are the *p*-phenylpyridinium and *p*-cyanopyridinium compounds, **2** and **3**, Scheme 4. The *p*-withdrawing group in **3R** limits the reaction rate as a result of the withdrawing effect. Withdrawing substituents in the *m*-position are expected to have a smaller negative electronic effect on the reaction barrier, and so the *m*-substituted **4** was chosen for this study in which faster fragmentation rates were sought. The *p*-phenyl group limits the reaction rate as a result of the delocalization effect, and so the *m*- and *o*-substituted compounds **5** and **6** were selected for study. A phenyl group in the *o*-position in **6** is expected to be less delocalizing than a *p*-phenyl substituent as a result of steric interaction with the *N*-methoxy group, which should cause the ring to be twisted out of conjugation with the pyridyl ring.

Finally, the orbital and state considerations clearly point to electron-donating groups in the *p*-position to decrease the electronic barrier to reaction, and so **7** and **8** were included in the present work to explore these effects. The *N*-ethyl compounds **9** and **10** were also required to model return electron transfer in the geminate pairs.

Kinetic Measurements

The goal is to identify bond fragmentation reactions that may occur at the fastest possible rates, and indeed, the fragmentation rate constants for the radicals studied here are all greater than 10^{10} s^{-1} , and some are greater than 10^{12} s^{-1} . Direct measurement of the rate constants requires the radicals to be formed faster than they react. Previously, excitation of charge-transfer (CT) complexes has been used to measure the rate constants for fast fragmentation reactions of this kind on the picosecond and, in a few cases, subpicosecond time scale.^{5,14,15} Several experimental issues related to these kinds of measurements, particularly the effect of solvent relaxation, have not been discussed previously, and so the method is described in some detail here.

The *N*-methoxypyridinium compounds of Scheme 4 are reasonably strong electron acceptors. Addition of a suitable one-electron donor, D, to a solution of the *N*-alkoxypyridinium results in the formation of a CT complex (see Supporting Information for an example). Excitation into the CT absorption band of this complex using a pulsed laser forms a donor radical cation/pyridyl radical pair within the time period of the excitation pulse. Subsequent reactions are those of the ($\text{D}^+ \text{X}-\text{Y}^\bullet$) geminate pair, Scheme 1.¹⁴

The important processes usually considered for geminate pairs of this type are return electron transfer to reform the ground-state CT complex, $k_{\text{-et}}$, and fragmentation of the radical, k_{fr} .^{14,15,20} Another process of geminate pairs, separation to form freely diffusing radicals in solution, is too slow for the particular systems studied here to appreciably compete with the other two.²⁰

The electronic absorptions in the visible region of the pyridyl radicals studied here are too weak to be observed in the presence of strong absorptions of the donor radical cation, D^+ .¹⁴ The kinetics of the pyridyl radicals are thus determined by monitoring D^+ . According to Scheme 1, the D^+ signal decays exponentially to a permanent value (on the ultrafast time scale) as a result of the removal of D^+ by the return electron-transfer reaction, $k_{\text{-et}}$. The permanent signal is a consequence of those pyridyl radicals that fragment within the geminate pair, thus avoiding return electron transfer. The observed rate constant for decay of D^+ is given by eq 2a. Here, A_0 is the absorbance of D^+ at time zero, and A_{inf} is the absorbance of the D^+ that does not decay on the ultrafast time scale. A quantum yield, Φ_{ions} , for formation of long-lived D^+ can be defined as in eq 2b. Values for the elementary rate constants $k_{\text{-et}}$ and k_{fr} are

- (20) (a) Gould, I. R.; Young, R. H.; Farid, S. *J. Phys. Chem.* **1991**, *95*, 2068. (b) Gould, I. R.; Young, R. H.; Farid, S. In *Photochemical Processes in Organized Molecular Systems*; Honda, K., Ed.; Elsevier: New York, 1991. (c) Gould, I. R.; Mueller, J. L.; Farid, S. *Z. Phys. Chem. (Munich)* **1991**, *170*, 143. (d) Gould, I. R.; Noukakis, D.; Gomez-Jahn, L.; Young, R. H.; Goodman, J. L.; Farid, S. *Chem. Phys.* **1993**, *176*, 439. (e) Arnold, B. R.; Noukakis, D.; Farid, S.; Goodman, J. L.; Gould, I. R. *J. Am. Chem. Soc.* **1995**, *117*, 4399. (f) Gould, I. R.; Farid, S. *Acc. Chem. Res.* **1996**, *29*, 522.

related to the observed rate constant for removal of $D^{\bullet+}$, k_{obs} , eq 2c, and are obtained as indicated in eqs 2d and 2e.

$$A(t) = (A_0 - A_{\text{inf}}) e^{-k_{\text{obs}}t} + A_{\text{inf}} \quad (2a)$$

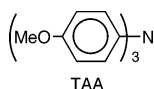
$$\Phi_{\text{ions}} = A_{\text{inf}}/A_0 \quad (2b)$$

$$k_{\text{obs}} = k_{-\text{et}} + k_{\text{fr}} \quad (2c)$$

$$k_{\text{fr}} = k_{\text{obs}} \Phi_{\text{ions}} \quad (2d)$$

$$k_{-\text{et}} = k_{\text{obs}} - k_{\text{fr}} \quad (2e)$$

Excitation of the CT complexes was performed using a femtosecond pump–probe laser system.²¹ According to eqs 2, the rate constant for fragmentation can only be determined with any accuracy if it competes appreciably with return electron transfer. If k_{fr} is much smaller than $k_{-\text{et}}$, then the yield of long-lived $D^{\bullet+}$ is small, and k_{fr} is a small fraction of the observed rate constant for geminate pair decay, k_{obs} . If k_{fr} is much larger than $k_{-\text{et}}$, then only a small decay as a function of time is observed, and k_{obs} cannot be determined accurately.^{5h,14,15} Because the fragmentation rate constants measured here were so large, very fast return electron transfer was necessary to compete appropriately. Return electron transfer occurs in the Marcus inverted region for radical ion pairs such as these,^{20,22} which means that the fastest reactions occur when the exothermicity of the return electron-transfer reaction is as small as possible. This requires the use of an electron donor D with as low an oxidation potential as possible. We have used *p*-trianisylamine (TAA) as the electron donor. The oxidation



potential of TAA is 0.52 V vs SCE.²² Amines with lower oxidation potentials than this are subject to atmospheric oxidation and are inconvenient to use. The $\text{TAA}^{\bullet+}$ has an absorption maximum at 715 nm in acetonitrile, with an extinction coefficient at this wavelength of 45,000.²² It thus represents an ideal choice for an electron donor.

Formation of CT complexes was readily observed between all of the pyridinium salts of Scheme 4 and TAA as the donor. Femtosecond excitation into the CT absorption bands at 410 nm resulted in transient absorptions in the region expected for $\text{TAA}^{\bullet+}$. Typical data are illustrated in Figures 2 and 3 for the *p*-phenylpyridyl radical, **2R**. After the pulse, absorption decay due to return electron transfer was observed to a constant level, as expected, except that the observed time-dependent absorption decays were different at different wavelengths. This was due to a change in the shape of the absorption band with time. The effect is illustrated in Figure 2. At early times an absorption maximum around 740 nm was observed, which had shifted to ca. 715 nm by the end of the decay time period. The latter wavelength is very close to that observed previously for $\text{TAA}^{\bullet+}$ in acetonitrile.²² The spectral shifts are assigned to time-

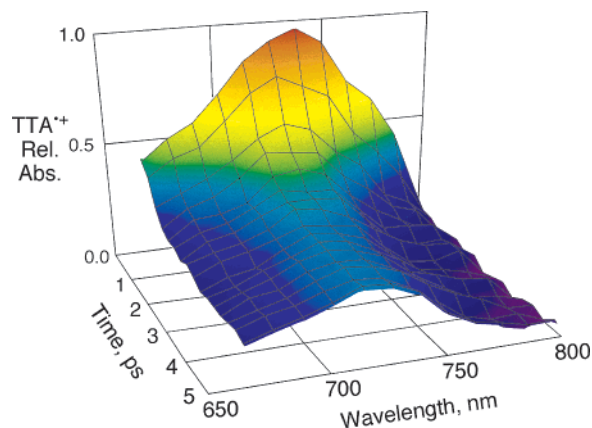


Figure 2. Absorption spectra as a function of time for excitation of the charge-transfer complex formed between *p*-trianisylamine (TAA) and *p*-phenyl-*N*-methoxyppyridyl tetrafluoroborate (**2**) in acetonitrile at room temperature, showing both decay and temporal evolution of the spectra from an absorbance maximum at ca. 740 nm to a maximum at ca. 715 nm.

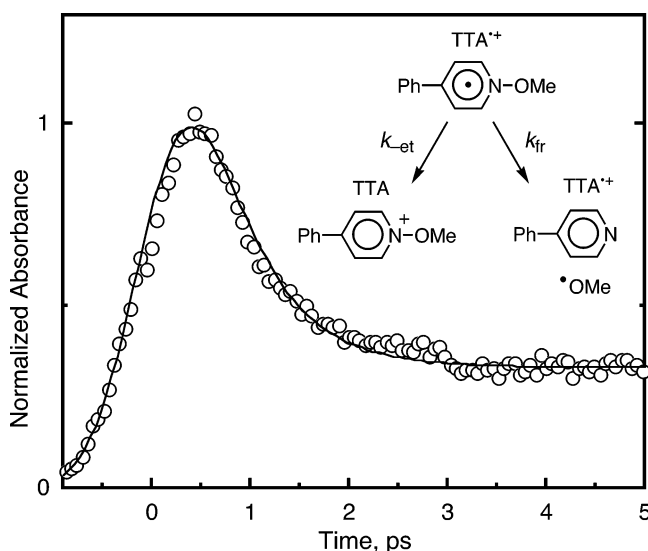


Figure 3. (○) Normalized absorbance of *p*-trianisylamine radical cation ($\text{TAA}^{\bullet+}$), integrated over the wavelength range 659–797 nm (see text) versus time for pulsed laser excitation at 410 nm of the charge-transfer complex formed between TAA and *p*-phenyl-*N*-methoxyppyridinium tetrafluoroborate (**2**) in acetonitrile at room temperature. The solid curve represents a fit to the data as described in the text and Experimental Section, using values for k_{obs} and Φ_{ions} of $1.8 \times 10^{12} \text{ s}^{-1}$ and 0.15, respectively, and a Gaussian instrument response function of 600 fs width. The values of k_{et} and k_{fr} obtained from these data (eqs 2) are 1.5×10^{12} and $2.7 \times 10^{11} \text{ s}^{-1}$, respectively.

dependent solvent relaxation around the geminate pair.²³ In small nitrile solvents these should occur roughly on a 1–2 ps time scale, as observed.^{23,24}

The time dependence of the concentration of the $\text{TAA}^{\bullet+}$ was determined by first correcting for the wavelength chirp of the


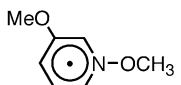
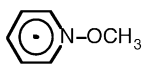
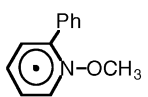
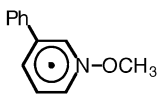
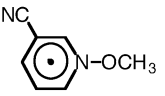
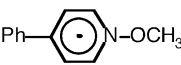
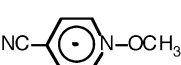
(21) Sakomura, M.; Lin, S.; Moore, T. A.; Moore, A. L.; Gust, D.; Fujihira, M. *J. Phys. Chem. A* **2002**, *106*, 2218.

(22) Gould, I. R.; Ege, D.; Moser, J. E.; Farid, S. *J. Am. Chem. Soc.* **1990**, *112*, 4290.

(23) (a) Johnson, A. E.; Levinger, N. E.; Kliner, D. A. V.; Tominaga, K.; Barbara, P. F. *Pure Appl. Chem.* **1992**, *64*, 1219. (b) Zeglinski, D. M.; Waldeck, D. H. *J. Phys. Chem.* **1988**, *92*, 692. (c) Maroncelli, M. *J. Mol. Liq.* **1993**, *57*, 1. (d) Fleming, G. R.; Cho, M. *Annu. Rev. Phys. Chem.* **1996**, *47*, 109. (e) Chang, Y. J.; Simon, J. D. *Springer Ser. Chem. Phys.* **1996**, *62*, 253. (f) Cramer, C. J.; Truhlar, D. G. *Chem. Rev.* **1999**, *99*, 2161.

(24) The change in solvation state during the time period of the processes being monitored should result in a time-dependent return electron-transfer rate constant and thus nonexponential kinetics. However, the change in the electron-transfer rate constant must be small, since we are able to fit the data well using the exponential eq 2a (see, for example, Figures 3 and 4). We assume that we are, in fact, measuring an averaged $k_{-\text{et}}$ that has a small distribution in values.

Table 1. Kinetic Parameters for Geminate Pairs of *N*-Methoxypyridyl Radicals and Radical Cations of *p*-Trianisylamine in Acetonitrile at Room Temperature

Structure	Radical	Φ_{ions}	$k_{\text{obs}}, \text{s}^{-1}$	$k_{\text{et}}, \text{s}^{-1}$	$k_{\text{fr}}, \text{s}^{-1}$
	7R	a	a	$>1.2 \times 10^{11}$ a	$>2.5 \times 10^{12}$ a
	8R	a	a	$>5.2 \times 10^{11}$ a	$>2.5 \times 10^{12}$ a
	1R	0.39	4.1×10^{12}	2.5×10^{12}	1.6×10^{12}
	6R	0.58	2.1×10^{12}	9.0×10^{11}	1.2×10^{12}
	5R	0.48	1.8×10^{12}	9.4×10^{11}	8.3×10^{11}
	4R	0.25	1.1×10^{12}	8.0×10^{11}	2.6×10^{11}
	2R	0.15 ^b	1.8×10^{12} b	1.5×10^{12} b	2.7×10^{11} b
	3R	b, c	b, c	b, c	1.2×10^{10} b, c

^a No decay of geminate pair observed; see text for discussion of these values. ^b Previously published data.¹⁴ ^c Not measured with TAA.¹⁴

white light probe beam^{21,25} and then integrating the absorbance band at the different time delays. A plot of this wavelength-corrected integrated absorbance versus time is shown in Figure 3, together with a fit to the data according to eq 2a, after convolution with a Gaussian instrument response function. Corresponding experiments were performed for the radicals **1R** and **4R–8R**, with the experimental data for **5R** and **6R** illustrated in Figure 4. Importantly, excitation of a CT complex of TAA with the *p*-methoxy and *m*-methoxy compounds **7** and **8** resulted in *no observable return electron transfer*, Figure 4 and Table 1. The kinetic parameters obtained by analyzing the time-resolved kinetic data according to eqs 2 for **1–8** are summarized in Table 1.

Mechanistic Implications

Our goal is the development of ultrafast fragmentation reactions that compete efficiently with return electron transfer. The rate constants for return electron transfer in the present cases are all very large, ca. 10^{12} s^{-1} (Table 1). The more efficiently the fragmentation reaction competes with return electron transfer, the higher the yield of long-lived TAA^{•+}, e.g., Figures 3 and 4. Note that the raw data shown in the figures are somewhat deceptive, since convolution effects make the apparent yields of long-lived TAA^{•+} absorption higher than the actual yields (Table 1). For all of the reactions studied here,

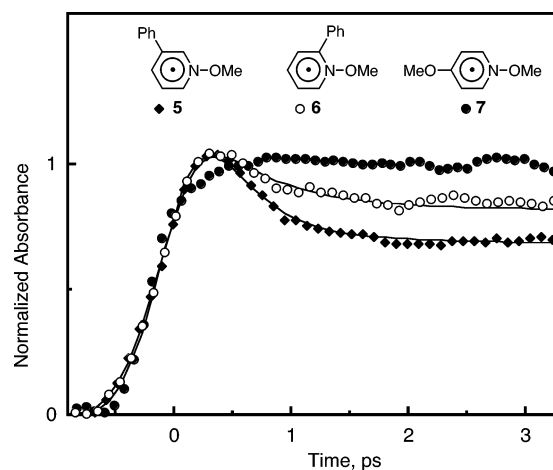


Figure 4. Normalized absorbance of *p*-trianisylamine radical cation, integrated over the wavelength range 659–797 nm (see text), versus time for pulsed laser excitation at 410 nm of the charge-transfer complexes formed between *p*-trianisylamine (TAA) and *p*-methoxy-*N*-methoxypyridinium tetrafluoroborate (**7**, ●), *m*-phenyl-*N*-methoxypyridinium tetrafluoroborate (**5**, ◆), and *o*-phenyl-*N*-methoxypyridinium tetrafluoroborate (**6**, ○) in acetonitrile at room temperature. The solid curves represent a fit to the data for **5** and **6** to eq 2a, as described in the text and Experimental Section, using values for the parameters given in Table 1. No fit is given for **7** because no decay is observed in this case.

however, fragmentation was sufficiently rapid that efficient formation of separated radicals occurs even with ultrafast return electron transfer.

(25) Yamaguchi, S.; Hamaguchi, H.-O. *Appl. Spectrosc.* **1995**, *49*, 1513.

The unsubstituted pyridyl radical **1R** turns out to be one of the fastest fragmenting radicals. As discussed above, delocalization of the spin in **2R** decreases the reaction rate. The effect of moving the phenyl from the para to the meta position (**5R**) is to increase the rate constant for fragmentation compared to **2R** by a factor of ca. 3. The phenyl group in the ortho position (**6R**) results in even faster fragmentation. In this case, steric interactions with the *N*-methoxy group cause the phenyl group to be sufficiently twisted that essentially no delocalization occurs.

The *p*-cyanopyridinium is the most useful radical precursor in a practical sense because the strong withdrawing group allows this compound to be reduced by the widest range of excited-state sensitizers. The para withdrawing group, however, results in the slowest reaction included here (**3R**, Table 1). We wondered if the strong withdrawing group could be retained in the structure, without the negative effect on the fragmentation rate constant. As with the *m*-phenyl radical above, the *m*-cyano radical **4R** reacts almost as fast as the unsubstituted parent radical.

The interesting observations are for the two methoxy-substituted radicals, **7R** and **8R**. The complete lack of return electron transfer observed for these radicals implies either extremely fast fragmentation, slow return electron transfer, or some combination of the two. In either case, fragmentation of the N–O bond occurs with no detectable energy-wasting return electron transfer, i.e., essentially 100% efficiency, but this observation alone is insufficient to determine whether the fragmentation reaction is barrierless. Furthermore, in the absence of observed return electron transfer, it is not possible to determine an absolute value for the rate constant for fragmentation. However, some reasonable limits can be set.

Two model compounds were studied, i.e., the corresponding *N*-ethyl-substituted compounds **9** and **10**, to obtain further information on the return electron-transfer process. Excitation of CT complexes of these acceptors with TAA results in immediate formation of a TAA⁺/pyridyl radical geminate pair as before. In this case, however, no bond fragmentation occurs, and only return electron transfer is observed.¹⁴ The return electron-transfer rate constants obtained for the radicals **9R** and **10R** with TAA⁺ are 1.2×10^{11} and 5.2×10^{11} s⁻¹, respectively. Simulations of the observed time-resolved absorptions for **7R** and **8R** were performed using the return electron-transfer rate constants for **9R** and **10R**, respectively, and various fragmentation rate constants. The best fits to the data are obtained using values for k_{fr} equal to or greater than 2.5×10^{12} s⁻¹ (details are given in Supporting Material). Furthermore, we previously found that return electron transfer in geminate pairs of the *N*-methoxy radicals was actually faster than in the corresponding *N*-ethyl radicals, presumably because the *N*-methoxy-substituted pyridiniums are easier to reduce than the *N*-ethylpyridiniums.¹⁴ The return electron-transfer rate constants for **9R** and **10R** above thus represent minimum values for corresponding return electron transfer in the **7R** and **8R** pairs. If return electron transfer in the **7R** and **8R** pairs is faster than in the **9R** and **10R** pairs, then the fragmentation rate constants are even higher than 2.5×10^{12} s⁻¹.

Thus, we estimate the lifetime for the radicals **7R** and **8R** to be probably less than 400 fs. The vibration frequency of the N–O bond in the reacting radicals is not known, and by

definition, a barrierless fragmentation reaction has no real vibration frequency along the bond-breaking coordinate. A maximum value can be obtained from the N–O bond stretching frequency of the parent pyridinium, for which a value of 390 cm⁻¹ can be estimated,²⁶ corresponding to a time constant of ca. 100 fs. The N–O bond must be weaker in the radical, corresponding to a vibrational time constant greater than 100 fs. Thus, the lifetime of the radicals **7R** and **8R** are determined to be a *maximum* of four vibrational periods and probably less. Although it is not possible to definitively say whether the reactions are barrierless or not, they are certainly very close, presumably as a consequence of the exothermicity and state splitting effects discussed above.

Summary

N–O bond fragmentation in *N*-methoxypyridyl radicals can occur on the subpicosecond time scale. The reaction is slowed by electron-withdrawing and electron-delocalizing groups. The way in which these substituents influence the fragmentation rate can be manipulated with steric effects and electronic effects and can be understood in terms of the important orbital and state correlations. Electron-donating groups increase the reaction rate close to the time scale for vibration of the fragmenting bond, and fragmentation of the *p*-methoxy-substituted radical may be barrierless.

Experimental Section

Materials. Acetonitrile was spectrograde (Omnisolv) and used as received. The *N*-methoxypyridinium compounds **2** and **3** were available from previous studies.¹⁴ General synthetic procedures for preparation of the *N*-methoxy and *N*-ethyl pyridiniums have been given previously.¹⁴ All of the pyridinium compounds were prepared and used as the tetrafluoroborate salts. *p*-Trianisylamine was a gift from D. Weiss (Eastman Kodak Company) and was used as received.

***N*-Methoxypyridinium Tetrafluoroborate (1).** Following the general procedure,¹⁴ trimethyloxonium tetrafluoroborate (3.48 g, 23.6 mmol) and pyridine *N*-oxide hydrate (2.00 g, 21.0 mmol) were stirred in 80 mL of dichloromethane for 4 h; 2.80 g (14.2 mmol, 68%) **1** was obtained as a colorless oil. ¹H NMR (300 MHz, CD₃CN): δ (ppm) 4.42 (s, 3 H), 8.14 (t, 2 H, *J* = 7.2 Hz), 8.57 (t, 1 H, *J* = 7.5 Hz), 9.01 (dd, 2 H, *J* = 1.2, 7.5 Hz). ¹³C NMR (75 MHz, CD₃CN): δ (ppm) 70.2, 130.0, 141.0, 145.7. MS *m/z*: 110.0 (M⁺).

***N*-Methoxy-3-cyanopyridinium Tetrafluoroborate (4).** Following the general procedure, trimethyloxonium tetrafluoroborate (0.72 g, 4.87 mmol) and 4-cyanopyridine *N*-oxide (0.56 g, 4.63 mmol) were stirred in 30 mL of dichloromethane for 4 h. Recrystallization from methanol afforded 0.81 g (3.65 mmol, 79%) of **4**. ¹H NMR (300 MHz, CD₃CN): δ (ppm) 4.53 (s, 3 H), 8.35 (dd, 1 H, *J* = 6.9, 8.1 Hz), 8.94 (dd, 1 H, *J* = 0.9, 6.6 Hz), 9.47 (d, 1 H, *J* = 5.9 Hz), 9.91 (s, 1 H). ¹³C NMR (75 MHz, CD₃CN): δ (ppm) 69.2, 114.5, 116.6, 129.4, 143.7, 144.4, 147.4. MS *m/z*: 135.1 (M⁺).

***N*-Methoxy-3-phenylpyridinium Tetrafluoroborate (5).** Following the general procedure,¹⁴ trimethyloxonium tetrafluoroborate (2.19 g, 14.8 mmol) and 3-phenylpyridine *N*-oxide (2.20 g, 12.8 mmol) were stirred in 40 mL of dichloromethane for 4 h. Recrystallization from methanol/dichloromethane afforded 3.38 g (12.4 mmol, 97%) of **5**. ¹H NMR (300 MHz, CD₃OH): δ (ppm) 3.14 (s, 3 H), 6.18 (d, 2 H, *J* = 1.8 Hz), 6.20 (d, 1 H, *J* = 2.1 Hz), 6.41–6.45 (m, 2 H), 6.80 (dd, 1 H, *J* = 6.6, 7.8 Hz), 7.40 (d, 1 H, *J* = 8.4 Hz), 7.72 (dt, 1 H, *J* = 0.9, 6.6 Hz), 8.08 (t, 1 H, *J* = 2.4 Hz). ¹³C NMR (75 MHz, CD₃OH): δ (ppm)

(26) This corresponds to the frequency of the normal mode that most approximates the N–O stretch from a B3PW91/6-31+G* computation on **7**. Details of these computations are given in: Lorance, E. D.; Hendrickson, K.; Gould, I. R. *J. Org. Chem.* Submitted for publication.

70.4, 118.2, 128.3, 130.0, 130.4, 131.4, 133.4, 139.3, 143.3, 143.7. MS m/z : 186.1 (M^+).

***N*-Methoxy-2-phenylpyridinium Tetrafluoroborate (6).** Following the general procedure,¹⁴ trimethyloxonium tetrafluoroborate (2.19 g, 14.8 mmol) and 2-phenylpyridine *N*-oxide (2.20 g, 12.8 mmol) were stirred in 40 mL of dichloromethane for 4 h. Recrystallization from methanol/dichloromethane afforded 3.3 g (12.1 mmol, 94%) of **6**. ¹H NMR (300 MHz, CD₃CN): δ (ppm) 4.01 (s, 3 H), 7.65–7.74 (m, 3 H), 7.80–7.84 (m, 2 H), 8.08–8.15 (m, 2 H), 8.55–8.60 (m, 1 H), 9.03 (d, $J = 5.1$ Hz, 1 H). ¹³C NMR (75 MHz, CD₃CN): δ (ppm) 69.7, 129.1, 129.4, 130.2, 131.0, 132.3, 133.3, 142.6, 146.5, 153.4. MS m/z : 186.1 (M^+).

***N*,4-Dimethoxypyridinium Tetrafluoroborate (7).** Following the general procedure,¹⁴ trimethyloxonium tetrafluoroborate (1.10 g, 7.43 mmol) and 4-methoxypyridine *N*-oxide hydrate (0.95 g, 6.64 mmol) were stirred in 30 mL of dichloromethane for 4 h; 0.81 g (4.24 mmol, 64%) of **7** was obtained as a colorless oil. ¹H NMR (300 MHz, CD₃CN): δ (ppm) 4.07 (s, 3 H), 4.27 (s, 3 H), 7.45 (d, 2 H, $J = 7.8$ Hz), 8.74 (d, 2 H, $J = 7.8$ Hz). ¹³C NMR (75 MHz, CD₃CN): δ (ppm) 62.4, 73.5, 121.8, 146.1, 174.9. MS m/z : 140.4 (M^+).

***N*,3-Dimethoxypyridinium Tetrafluoroborate (8).** Following the general procedure,¹⁴ trimethyloxonium tetrafluoroborate (1.10 g, 7.43 mmol) and 4-methoxypyridine *N*-oxide hydrate (0.95 g, 6.64 mmol) were stirred in 30 mL of dichloromethane for 4 h; 0.81 g (4.24 mmol, 64%) of **8** was obtained as a colorless oil. ¹H NMR (300 MHz, CD₃CN): δ (ppm) 3.42 (s, 3 H), 3.82 (s, 3 H), 7.44–7.49 (m, 1 H), 7.56–7.60 (m, 1 H), 8.36 (m, 1 H), 8.62 (m, 1 H). ¹³C NMR (75 MHz, CD₃CN): δ (ppm) 58.0, 70.0, 129.0 (2 C), 130.8, 133.3, 159.5. MS m/z : 140.2 (M^+).

***N*-Ethyl-4-methoxypyridinium Tetrafluoroborate (9).** Following the general procedure,¹⁴ triethyloxonium hexafluorophosphate (4.8 g, 18.8 mmol) and 3-methoxypyridine (1.43 g, 1.3 mL, 13.0 mmol) were stirred in 30 mL of dichloromethane for 4 h; 3.38 g (11.9 mmol, 91%) of **9** was obtained as a colorless oil. ¹H NMR (300 MHz, CD₃CN): δ (ppm) 1.57 (t, 3 H, $J = 7.8$ Hz) 4.13 (s, 3 H), 4.47 (q, 2 H, $J = 7.8$ Hz), 7.48 (d, 2 H, $J = 7.8$ Hz), 8.65 (d, 2 H, $J = 7.8$ Hz). ¹³C NMR (75 MHz, CD₃CN): δ (ppm) 16.3, 56.4, 58.5, 113.4, 146.6, 172.7. MS m/z : 138.2 (M^+).

***N*-Ethyl-3-methoxypyridinium Tetrafluoroborate (10).** Following the general procedure,¹⁴ triethyloxonium hexafluorophosphate (2.60 g, 11.5 mmol) and 3-methoxypyridine (1.43 g, 1.3 mL, 13.0 mmol) were stirred in 30 mL of dichloromethane for 4 h; 2.58 g (9.1 mmol, 79%) of **10** was obtained as a colorless solid. ¹H NMR (300 MHz, CD₃CN): δ (ppm) 1.58 (t, 3 H, $J = 7.8$ Hz) 3.99 (s, 3 H), 4.52 (q, 2 H, $J = 7.8$ Hz), 7.88–7.92 (m, 1 H), 7.98–8.03 (m, 1 H), 8.28–8.32 (m, 1 H), 8.36–8.38 (m, 1 H). ¹³C NMR (75 MHz, CD₃CN): δ (ppm) 16.6, 58.3, 56.4, 129.7, 131.4, 133.0, 137.5, 159.9. MS m/z : 138.2 (M^+).

Ultrafast Transient Absorption Experiments. The laser apparatus has been described previously.²¹ Experiments were performed in 1-cm³ cuvettes with continuous stirring. The concentrations of the *p*-trianisylamine and the *N*-methoxypyridinium compounds were adjusted

to give an optical density close to 1.0 at the laser excitation wavelength. Typically the amine concentration was about 0.06 M, and the methoxypyridinium compounds were about 0.3 M. The laser repetition rate was 10 kHz, and to avoid buildup of too high a concentration of the TAA radical cation (which would excessively attenuate the probe beam), ca. 0.05 M triethylamine was added to reduce this species back to the neutral TAA between pulses. Experiments performed in the presence and absence of triethylamine showed no difference in the kinetics of the geminate pairs (except that the solutions had to be replaced more frequently in the absence of the TEA). The presence of the TEA also did not affect the absorption of the CT complexes formed between the *N*-methoxypyridinium compounds and the TAA. The time-resolved absorbance spectral data was corrected for chirp in the probe beam using the method described previously.²¹ The corrected absorbance spectra were integrated over the range 659–797 nm. The resulting data were fitted to eq 2a after convolution of the equation with a Gaussian instrument response function. The width of the Gaussian was a fitting factor and was typically ca. 600 fs. In some cases a small (less than 10%) additional exponential component was required to obtain a good fit to the data, with an ill-defined time constant from 10 to 100 ps. Although not accurately determined, this long time constant is clearly not related to the dynamics of the geminate amine radical cation/pyridyl radical pairs, which are much shorter lived, and is assigned to decay of a small amount of amine radical cation formed by two-photon ionization of uncomplexed amine, which presumably decays by reaction with solvated electrons. Experiments conducted with only trianisylamine and with trianisylamine and triethylamine gave similar spectra and decay times.

Errors in the various rate constants were estimated from repeated measurements and are different for the different radicals. The errors on the rate constants for fragmentation are somewhat higher for those radicals with yields of ions that were particularly high or low. A maximum error of ca. 25% is estimated for the rate constants in each case.

Acknowledgment. A research grant from The Research Corporation is gratefully acknowledged. The authors thank J. P. Dinnocenzo (University of Rochester) for several helpful discussions and J. T. Hynes (University of Colorado, Boulder) for preprints of his work on related fragmentation reactions. Instrumental support from the ASU Center for the Study of Early Events in Photosynthesis is acknowledged.

Supporting Information Available: Absorption spectrum of a typical charge-transfer complex and simulations of the time-resolved absorption data for the *m*-methoxy-*N*-methoxypyridyl (**8R**) and *p*-methoxy-*N*-methoxypyridyl (**7R**) radicals. This material is available free of charge via the Internet at <http://pubs.acs.org>.

JA030438+